

DTIC FILE COPY

AFGL-TR-88-0248

2

AD-A201 003

A Simple Solar Microwave Burst
Observed With High Spectral Resolution

Dale E. Gary
G.J. Hurford

California Institute of Technology
Big Bear Solar Observatory
Pasadena, CA 91125

August 1988

Scientific Report No. 1

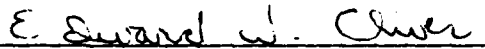
APPROVED FOR PUBLIC RELEASE; DISTRIBUTION UNLIMITED

AIR FORCE GEOPHYSICS LABORATORY
AIR FORCE SYSTEMS COMMAND
UNITED STATES AIR FORCE
HANSCOM AIR FORCE BASE, MASSACHUSETTS 01731

DTIC
ELECTE
OCT 17 1988
S H D

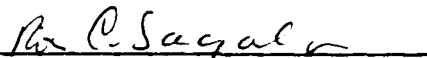
88 1017 001

"This technical report has been reviewed and is approved for publication"


EDWARD W. CLIVER
Contract Manager


WILLIAM J. BURKE
Branch Chief

FOR THE COMMANDER


R.C. SAGALYN
Division Director

This report has been reviewed by the ESD Public Affairs Office (PA) and is releasable to the National Technical Information Service (NTIS).

Qualified requestors may obtain additional copies from the Defense Technical Information Center. All others should apply to the National Technical Information Service.

If your address has changed, or if you wish to be removed from the mailing list, or if the addressee is no longer employed by your organization, please notify AFGL/DAA, Hanscom AFB, MA 01731-5000. This will assist us in maintaining a current mailing list.

Do not return copies of this report unless contractual obligations or notices on a specific document requires that it be returned.

REPORT DOCUMENTATION PAGE

1a. REPORT SECURITY CLASSIFICATION Unclassified			1b. RESTRICTIVE MARKINGS		
2a. SECURITY CLASSIFICATION AUTHORITY			3. DISTRIBUTION/AVAILABILITY OF REPORT Approved for public release; Distribution unlimited		
2b. DECLASSIFICATION/DOWNGRADING SCHEDULE					
4. PERFORMING ORGANIZATION REPORT NUMBER(S)			5. MONITORING ORGANIZATION REPORT NUMBER(S) AFGL-TR-88-0248		
6a. NAME OF PERFORMING ORGANIZATION California Institute of Technology		6b. OFFICE SYMBOL (if applicable)	7a. NAME OF MONITORING ORGANIZATION Air Force Geophysics Laboratory		
6c. ADDRESS (City, State, and ZIP Code) Big Bear Solar Observatory Pasadena, CA 91125			7b. ADDRESS (City, State, and ZIP Code) Hanscom AFB Massachusetts 01731-5000		
8a. NAME OF FUNDING/SPONSORING ORGANIZATION		8b. OFFICE SYMBOL (if applicable)	9. PROCUREMENT INSTRUMENT IDENTIFICATION NUMBER F19628-86-K-0017		
8c. ADDRESS (City, State, and ZIP Code)			10. SOURCE OF FUNDING NUMBERS		
			PROGRAM ELEMENT NO. 61102F	PROJECT NO. 2311	TASK NO. G3
			WORK UNIT ACCESSION NO. DM		
11. TITLE (Include Security Classification) A Simple Solar Microwave Burst Observed With High Spectral Resolution					
12. PERSONAL AUTHOR(S) Dale E. Gary; G.J. Hurford					
13a. TYPE OF REPORT Scientific Report #1		13b. TIME COVERED FROM _____ TO _____		14. DATE OF REPORT (Year, Month, Day) 1988 August	15. PAGE COUNT
16. SUPPLEMENTARY NOTATION					
17. COSATI CODES			18. SUBJECT TERMS (Continue on reverse if necessary and identify by block number)		
FIELD	GROUP	SUB-GROUP	Sun: radio radiation Sun: X-rays Sun: flares		
			Sun: corona Sun: structure		
19. ABSTRACT (Continue on reverse if necessary and identify by block number)					
<p>Many solar microwave bursts exhibit multicomponent spatial and spectral structure, which complicates efforts to determine source parameters from their radio emission. We analyze a small (SN/C1.0) flare that occurred on 1986 February 3, dominated by a single, homogeneous source. High spectral resolution observations of this event with the Owens Valley frequency-agile interferometer therefore provide the clearest opportunity to date to apply theoretical spectral models to a microwave burst. Based on the microwave spectra, we find that the burst was dominated by a compact, thermal source. The sequence of such spectra, obtained every 10 s, showed that the source expanded with time during the burst, starting with a (one-dimensional) size of 4 arcsec, enlarging to ~12 arcsec in <2 minutes. During the</p>					
20. DISTRIBUTION/AVAILABILITY OF ABSTRACT <input type="checkbox"/> UNCLASSIFIED/UNLIMITED <input type="checkbox"/> SAME AS RPT <input type="checkbox"/> DTIC USERS			21. ABSTRACT SECURITY CLASSIFICATION Unclassified		
22a. NAME OF RESPONSIBLE INDIVIDUAL Edward Cliver			22b. TELEPHONE (Include Area Code)	22c. OFFICE SYMBOL AFGL/PHP	

same period, the electron temperature decreased from a high of 7.1×10^7 K to $<10^7$ K. Comparison with GOES soft X-ray data suggests that the density increased by at least an order of magnitude during the burst. The magnetic field strength was found to be ~ 770 G. To apply these techniques to typical, more inhomogeneous flares, future observations are needed that achieve better imaging capability while retaining high spectral resolution.

2/10/74



Accession For	
NTIS GRA&I	<input checked="" type="checkbox"/>
DTIC TAB	<input type="checkbox"/>
Unannounced	<input type="checkbox"/>
Justification	
By	
Distribution/	
Availability Codes	
Dist	Avail and/or Special
A-1	

A SIMPLE SOLAR MICROWAVE BURST OBSERVED WITH HIGH SPECTRAL RESOLUTION

DALE E. GARY and G. J. HURFORD

Big Bear Solar Observatory, California Institute of Technology

ABSTRACT

Many solar microwave bursts exhibit multicomponent spatial and spectral structure, which complicates efforts to determine source parameters from their radio emission. We analyze a small (SN/C1.0) flare that occurred on 1986 February 3, dominated by a single, homogeneous source. High spectral resolution observations of this event with the Owens Valley frequency-agile interferometer therefore provide the clearest opportunity to date to apply theoretical spectral models to a microwave burst. Based on the microwave spectra, we find that the burst was dominated by a compact, thermal source. The sequence of such spectra, obtained every 10 s, showed that the source expanded with time during the burst, starting with a (one-dimensional) size of 4 arcsec, enlarging to ~ 12 arcsec in < 2 minutes. During the same period, the electron temperature decreased from a high of 7.1×10^7 K to $< 10^7$ K. Comparison with GOES soft X-ray data suggests that the density increased by at least an order of magnitude during the burst. The magnetic field strength was found to be ~ 770 G. To apply these techniques to typical, more inhomogeneous flares, future observations are needed that achieve better imaging capability while retaining high spectral resolution.

Subject Headings: Sun : radio radiation — Sun : X-rays — Sun : flares —
Sun : corona — Sun : structure

I. INTRODUCTION

The bulk of the emission generated in the microwave region of the solar radio spectrum is due to incoherent continuum radiation from electrons accelerated in the solar corona. The spectral characteristics of this continuum emission have been well studied for a variety of emission mechanisms and electron energy distributions (e.g., Ramaty 1969; Takakura and Scalise 1970). Recent work has centered around simplifying the often complicated expressions for ranges of validity important for solar emission (Dulk and Marsh 1982; Robinson and Melrose 1984; Dulk 1985). The spectra one obtains from these expressions are strictly valid only for homogeneous sources, i.e., ones in which the plasma and electron parameters do not vary appreciably within the source.

In the literature one finds reports that observed spectra do not fit the theoretically expected spectra from homogeneous sources. Total power spectra, those without spatial resolution, are often flatter than expected, presumably due to gradients in density, magnetic field, etc., within the source (Dulk and Dennis 1982; Crannell *et al.* 1988). For some bursts, part of the problem may lie in the use of observations at a small number of widely spaced frequencies to define the spectrum (see Stähli, Gary and Hurford 1988). However, burst observations with good spectral coverage show other evidence of inhomogeneity, such as multiple spectral components (Stähli, Gary and Hurford 1988; Gary and Hurford 1988). Imaging data at multiple frequencies with the VLA sometimes show multiple spatial and spectral components as well (Shevgaonkar and Kundu 1985; Dulk, Bastian, and Kane 1986). The conclusion is inescapable that many solar bursts arise from inhomogeneous and/or multiple sources.

This complexity complicates the quantitative application of microwave theory to typical bursts. The purpose of this paper is to compare theoretical spectra with high spectral resolution observations of a particularly simple burst. In Section II, we demonstrate the simple nature of the burst by examination of its spectral, spatial, and temporal characteristics. In Section III, we analyze the data to obtain such physical parameters as electron temperature, source size, magnetic field strength, and electron density, all as a function of time. Conclusions are presented in Section IV.

II. A SIMPLE BURST

The flare occurred in NOAA region AR4711 on 1986 February 3, reaching maximum at ~ 1804 UT. It was reported as SF/SN in $H\alpha$, C1.0 in soft X-rays, and displayed two short lived $H\alpha$ kernels. The event was observed with the frequency-agile interferometer at the Owens Valley Radio Observatory (OVRO), described by Hurford, Read, and Zirin (1984). Operating in its two-element mode, with 27 m diameter antennas deployed on a xxx m east-west baseline, interferometric observations were obtained at 45 frequencies distributed

approximately logarithmically between 1 and 18 GHz in both right and left circular polarization. Since the frequency-agile system cycles rapidly (once every 10 seconds) through the frequencies and polarizations the system functioned in effect as a microwave spectrometer. Amplitudes were calibrated with respect to 3C84 which in turn was calibrated with respect to 3C286.

Figure 1 shows the time profile of the burst at two frequencies near the spectral peak. In this and following figures, crosses denote right hand (RH) circular polarization and boxes denote left hand (LH) polarization. The burst has a simple profile in time and circular polarization, being unpolarized below ~ 10 GHz and highly RH circularly polarized above 10 GHz. The microwave burst was unusual in that it was confined to high frequencies with a peak flux density of about 25 solar flux units (SFU) at 13 GHz, while scarcely reaching 1 SFU at 5 GHz. The simple temporal structure and short duration of the burst are characteristic of X-ray type A bursts (Dennis 1988 and references therein). Although not observed in hard X-rays, we shall see below that the burst fits other characteristics of type A bursts; it is spatially compact, and is due to a thermal distribution of electrons.

Figure 2 shows burst spectra in total power at 6 representative times, overlotted with thermal spectral fits for right- and left-hand circular polarization. The fitting procedure is described in Stähli, Gary, and Hurford (1988), and is only briefly outlined here. The least-squares procedure fits the functional form

$$S_{sfu} = A\nu^a(1 - e^{-B\nu^{-b}})$$

where a corresponds to the low-frequency slope of the spectrum, and $a - b$ corresponds to the high-frequency slope. Two other measurable quantities, peak flux and peak frequency, are combinations of the four fit parameters. Because the low-frequency slope is close to that expected for a homogeneous thermal burst, we fixed the low-frequency slope at +2, so that only three parameters are allowed to vary; maximum flux, peak frequency, and high frequency slope. The right and left circular polarizations were fit separately. As is evident from Figure 2, a thermal fit is a very good approximation throughout the burst. A second spectral component is apparent near 4.5 GHz, but is a minor constituent of the burst and will be ignored in the following discussion.

Further evidence of the simple nature of the burst can be seen by examining the correlated amplitude and phase from the OVRO interferometer. As discussed by Gary and Hurford (1988), the relative visibility spectrum (the ratio of the fringe amplitude to the total power as a function of frequency) is a convenient measure of complexity. In addition, the relative visibility spectrum can be used as a very sensitive measure of the (one-dimensional) size of the burst source. Figure 3 shows relative visibility spectra at three times early in the burst. A single, Gaussian source will have a relative visibility near unity at low frequencies, but at higher frequencies the decreasing fringe spacing will cause the source to become increasingly over-resolved. Thus, the relative visibility spectrum will have a well specified shape that

depends only on the source size. As Figure 3 shows, the source for this burst had a relative visibility spectrum consistent with a source ~ 4.5 arcsec in size at 180340 UT (just before the maximum of the burst), increasing to about ~ 6 arcsec at the maximum, and further increasing to ~ 7.5 arcsec during the decay. Note that the behavior seen in Figure 3 can be explained only if the source is a single, simple, compact source. If the source size varied with frequency, the shape of the relative visibility curves would be correspondingly different. (See Gary and Hurford (1988) for some contrasting examples of the relative visibility of complex sources.)

Figure 4 shows a high resolution off-band $H\alpha$ image obtained at Big Bear Solar Observatory. Overlaid on the $H\alpha$ image is a one-dimensional map made from the OVRO data by employing the technique of frequency synthesis (Hurford and Gary 1986; Gary and Hurford 1988). The map is based upon the relative visibility spectrum and the interferometer phase data. The use of the relative visibility spectrum is equivalent to normalizing (weighting) the fringe amplitude spectrum by the total power spectrum. It is apparent that the source location determined from the OVRO frequency synthesis map fits very well to the location of the $H\alpha$ kernels. Since such maps are most sensitive to the phase data, this provides independent evidence that the burst is a simple, single source.

We conclude that the burst was an unusually simple, homogeneous, thermal flare, probably of type A. In the next section, we apply the theory of thermal gyrosynchrotron emission from a homogeneous source to determine the important plasma and electron parameters.

III. PARAMETERS OF THE BURST

a) Source Size and Temperature

For thermal microwave emission, the electron temperature can be unambiguously determined from the brightness temperature of the emission in the optically thick portion of the spectrum. The brightness temperature, T_b , is related to the flux density, S , by

$$T_b = \frac{Sc^2}{k\nu^2 \Delta\Omega} = 2.775 \times 10^{10} \frac{S_{\text{sfu}}}{\pi(d^2/4) \nu_{\text{GHz}}^2} \quad (1)$$

where k is Boltzmann's constant, $\Delta\Omega$ is the angular area of the source, c is the speed of light, ν_{GHz} is the observing frequency (GHz), S_{sfu} is the flux density (solar flux units), and d is the one-dimensional source size (arcsec). In the optically thick portion of the spectrum, the electron temperature is just

$$T_e = T_b \quad (\tau \gg 1) \quad (2)$$

where τ is the optical depth.

The one-dimensional source size, d , has been determined from the relative visibility spectra, as in Figure 3, for each 10 s from 180330-180630 UT. Application

of equations (1) and (2) then give the electron temperature as a function of time under the assumption that the source has a gaussian cross-section of FWHM diameter d . Of course, the source could have any size in the direction along the fringes, but it is unlikely that the error is more than a factor of ~ 2 . Figure 5 shows time profiles of the source size d and the electron temperature T_e during the main part of the burst. From the figure, we see that the burst expanded steadily by about a factor of 3 in its linear dimension, while the electron temperature was first measured near 2.5×10^7 K, increased slightly to 7.1×10^7 K, and then decreased steadily thereafter.

Although the burst was not observed in hard X-rays, soft X-ray data from the GOES spacecraft are available. The plasma temperature and emission measure can be determined from GOES data by following the procedure of Thomas, Starr, and Crannell (1985); a comparison of the GOES and OVRO data is of interest. The GOES temperature and emission measure for this event are plotted in Figure 6, with the OVRO temperature from Figure 5 shown for comparison. Early in the flare, the temperatures do not match; the GOES temperature never much exceeds 10^7 K, although GOES should be sensitive to temperatures up to $\sim 3 \times 10^7$ K. A possible explanation is that the soft X-ray emission, which is a density weighted quantity, is dominated by the large emission measure of relatively low temperature plasma while the microwave emission, which depends only very weakly on density, more closely follows the peak temperature. On this interpretation, the emission measure of the high temperature (7×10^7 K) plasma seen in microwaves must be at least an order of magnitude less than that at 10^7 K (i.e., $\leq 10^{46}$ cm $^{-3}$), else it would have been visible in soft X-rays.

After about 180540, when the the GOES emission measure has reached its maximum and the cooling trend of the OVRO temperature has ended, the two temperatures agree to within 30 percent. This is about the level of agreement that might be expected, particularly when one considers the assumption of circular symmetry in the OVRO estimate.

b) Magnetic Field Strength and Electron Density

For thermal gyrosynchrotron emission, the peak frequency, ν_{peak} , of the radio spectrum is determined primarily by the magnetic field strength, B , in the thermal plasma, with a weaker dependence on dependence on angle of B to the line of sight, θ , and on the product of electron density, N , and line of sight depth, L , in the radio source (see Dulk 1985). In determining B , the corrections for θ and NL can be made as follows. We determine the angle, θ , from the observed polarization whose value of $\sim 50\%$ in this case requires $\theta > 80^\circ$ for $T_e < 10^8$ K (cf. Dulk 1985, Fig. 3f). We adopt $\theta = 85^\circ$, but note that subsequent results are insensitive to the exact value of θ when $\theta > 80^\circ$.

Next, we can make use of the GOES data to remove the weak NL dependence of ν_{peak} . From Figure 6 we see that the OVRO and GOES temperatures agree at

about 180510 UT, when the GOES emission measure peaks. If we assume that the GOES volume is the same as the OVRO source volume at this time, and further assume that the OVRO volume is $\sim d^3$, where d is the measure of source size shown in Figure 5, then the GOES emission measure can be used to estimate the OVRO column density

$$NL \approx \sqrt{EM/d} \quad (3)$$

where EM is the GOES emission measure (cm^{-3}). With these assumptions, the deduced value of NL at 180510 UT is $\sim 3.7 \times 10^{19} \text{ cm}^{-2}$, or, since $L = d$, $N \sim 5 \times 10^{10} \text{ cm}^{-3}$. At this time, then, we have estimates for N , L , T , and θ , and can determine B uniquely from the observed peak frequency, ν_{peak} . Unfortunately, the simple expression given by Dulk (1985) is not valid below $T_e = 10^7 \text{ K}$, and is not suitable for following the time behavior of the peak frequency, to the accuracy required, as the temperature falls to below 10^7 K . We determined the dependence of ν_{peak} on these parameters from numerical calculations based on the formulation of Ramaty (1969), using code kindly provided by G. A. Dulk. Figure 7 shows one result of these calculations. Shown is the dependence of ν_{peak} on B for both x-mode (solid, angled line) and o-mode (dashed, angled line), using the parameters known at 180510 UT. Superimposed on the plot are the observed peak frequencies for the two polarizations (vertical lines). Where these lines cross (dots), the indicated B value is noted. The values obtained independently for the two polarizations agree within about 5 percent. The average result of 770 G requires that the thermal gyrosynchrotron emission occur at low harmonics of the gyrofrequency (5-6).

At other times, when the assumption of identical soft X-ray and radio volumes cannot be verified, the microwave data alone cannot be used to determine N and B separately. However, the numerical calculations mentioned above indicate how ν_{peak} depends on the combination of these parameters. We find that the allowed combinations of B and N lie along different curves at different times, as shown in Figure 8. Because ν_{peak} and T_e decrease with time, the curves are displaced, each lying to the upper right of the one before. The actual values of B and N are constrained to lie on these curves at the corresponding times. The values of B and N at 180510 UT are known, and marked with a dot on Figure 8. This provides an additional constraint; the evolution of the values of B and N trace a path that must pass through this point. If we assume that B is constant, then the evolutionary path follows the arrow shown in the figure. In this case, the density must increase by more than three orders of magnitude in order to explain the observed slight shift in ν_{peak} . The magnitude of the change in density can only be reduced if we allow B to increase during the burst. If B decreases, the change in N will be even larger.

The picture that emerges, then, is that a thermal population of electrons is accelerated in a compact (~ 4 arcsec) source of rather high magnetic field strength ($\sim 770 \text{ G}$). The electrons emit microwaves due to thermal gyrosynchrotron emission at rather low harmonics of the gyrofrequency ($\sim 5-6$). The source expands slowly with time ($\sim 60 \text{ km s}^{-1}$), and the temperature decreases while the density increases

greatly, perhaps due to chromospheric evaporation (Bruner *et al.* 1988).

IV. DISCUSSION AND CONCLUSION

This demonstratively simple burst has given us a rare opportunity to apply the theory of microwave emission from homogeneous sources in order to follow the evolution of the burst. The spectral profile unambiguously indicates a thermal origin. The detailed spectral shape and polarization structure expected from thermal homogeneous sources is fully confirmed in this burst, without the need for further absorption processes or unusual electron energy profiles, pitch angle distributions, and the like. The parameters of the fits (corresponding to peak flux and peak frequency) gave plausible values for plasma temperature as a function of time, with the temperatures so obtained representing the peak temperature of a multithermal plasma, as distinct from the more familiar emission-measure sensitivity of soft X-rays. For the thermal plasma, the peak frequency of the microwave spectra depend on a combination of B and NL . By combining GOES and microwave spatial data we were able to eliminate the NL dependence and obtain values of magnetic field in the thermal source that are consistent to 5 percent in the two senses of circular polarization. The polarization of the microwave data gave the orientation of this 770 G field to the line-of-sight. Frequency-synthesis using the two-element data indicate a location for this single thermal source consistent with overlying the $H\alpha$ footpoints. In summary, conventional theoretical models can fit this demonstratively simple burst very well, and the result of the fits give a plausible set of plasma and field parameters.

Despite the successes of this application of the theory, we point out that this study has several drawbacks. A major problem is the lack of knowledge of the size of the source in the other dimension, parallel to the interferometer fringes. This uncertainty causes a directly proportional uncertainty in the derived temperature and may account for much of the 30 percent discrepancy between the late-stage GOES and microwave temperature estimates. Furthermore, with present instrumentation, the techniques used can only be applied with confidence to bursts that are spatially and spectrally homogeneous. Such bursts tend to be relatively rare and limited to small events. To apply these techniques to more typical flares, future observations are needed that achieve better imaging capability while retaining high spectral resolution.

Acknowledgements: We thank B. R. Dennis for drawing our attention to the usefulness of the GOES data. We also thank G. A. Dulk for making his numerical code for gyrosynchrotron emission available to us, and M. Stähli for stimulating discussions. This work has benefitted greatly from the dedication of our observer, D. Daugherty. This work was supported by NSF grants ATM-8610330 and AST-8702682, AFGL contract F19628-86-K-0017 and by NASA grant NAG 5-946.

REFERENCES

- Bruner, M. E., Crannell, C. J., Goetz, F., Magun, A., and McKenzie, D. L. 1988, *Ap. J.* in press.
- Crannell, C. J., Dulk, G. A., Kosugi, T., and Magun, A. 1988, *Solar Phys.*, submitted.
- Dennis, B. R. 1985, *Solar Phys.*, 150, 465.
- Dennis, B. R. 1988, *Solar Phys.*, submitted.
- Dulk, G. A. 1985, *Ann. Rev. Astron. Astrophys.*, 23, 169.
- Dulk, G. A., Bastian, T. S., and Kane, S. R., *Ap. J.*, 300, 438.
- Dulk, G. A., and Dennis, B. R. 1982, *Ap. J.*, 260, 844.
- Dulk, G. A., and Marsh, K. A. 1982, *Ap. J.*, 259, 350.
- Gary, D. E., and Hurford, G. J. 1988, in preparation.
- Hurford, G. J., and Gary, D. E. 1986, *Bull. AAS*, 18, 899.
- Hurford, G. J., Read, R. B., and Zirin, H. 1984, *Solar Phys.*, 94, 413.
- Ramaty, R. 1969, *Ap. J.*, 158, 753.
- Robinson, P. A., and Melrose, D. B. 1984, *Aust. J. Phys.*, 37, 675.
- Shevgaonkar, R. K., and Kundu, M. R. 1985, *Ap. J.*, 292, 733.
- Stähli, M., Gary, D. E., Hurford, G. J. 1988, in preparation.
- Takakura, T., and Scalise, E., Jr. 1970, *Solar Phys.*, 11, 434.
- Thomas, R. J., Starr, R., and Crannell, C. J. 1985, *Solar Phys.*, 95, 323.

Figure Captions

Figure 1.

Time profiles of the burst at two frequencies near the spectral peak. In this and other figures, crosses denote right hand (RH) circular polarization and boxes denote left hand (LH) polarization. Note the simple temporal and polarization structure. At 9.4 GHz (top panel), both senses of circular polarization are optically thick and the fluxes agree. At the slightly higher frequency of 11.2 GHz (bottom panel), the RH polarization remains optically thick, while LH has become optically thin.

Figure 2.

Log scale plots of total power spectra in RH and LH circular polarization, for 6 representative times during the burst. Superimposed on the observed spectra are model fits assuming thermal gyrosynchrotron emission from a homogeneous source. The fits are consistent with the data except for the presence of a separate, minor spectral component below ~ 6 GHz.

Figure 3.

Plot of relative visibility as a function of frequency for three times near the peak of the burst, overplotted with the expected form for sources of various sizes. At higher frequencies, the smaller interferometer fringe spacing results in greater over-resolution of the source, causing a drop in relative visibility. The amount of over-resolution increases as the source size increases. The data show that the (one-dimensional) size of the source increases steadily with time.

Figure 4.

High resolution $H\alpha$, -0.7 \AA off-band image taken at 180431 UT at Big Bear Solar Observatory. Superimposed on the image are grid lines of solar longitude and latitude, and an OVRO frequency synthesis (one-dimensional) map obtained from data taken at 180410 UT. The OVRO data are consistent with a compact, single source overlying the $H\alpha$ footpoints. Unfortunately, no information is available on the size of the source in the other dimension, along the fringes.

Figure 5.

Evolution of one-dimensional source size, d , determined as shown in Fig. 3, and the derived temperature in RH and LH circular polarization, assuming that the area of the radio source is $\pi d^2/4$. After 1806 UT, the decreasing flux made the size determination unreliable.

Figure 6.

Evolution of temperature and emission measure derived from GOES soft X-ray data (solid lines) compared with the evolution of OVRO temperature from Fig. 5. The two temperatures agree at about the time the GOES emission measure (EM) peaks. This may be because the density weighted soft X-ray flux is dominated by 10^7 K plasma, while the OVRO flux is dominated by higher temperature material with much smaller emission measure, as explained in the text.

Figure 7.

Dependence of the spectral peak frequency, ν_{peak} , on magnetic field strength for both x-mode (solid, angled line) and o-mode (dashed, angled line), for the values of N , L , and T determined at 180510 UT. The vertical lines represent the observed values of ν_{peak} for RH (solid) and LH (dashed) circular polarization. The value of B can be read directly from the vertical axis at the points where the solid and dashed lines cross. The corresponding values of B agree to within about 40 G for the two polarizations.

Figure 8.

Combination of values of B and N at various times, calculated from numerical expressions based on Ramaty (1969), using the observed ν_{peak} and deduced T_e and L . The curves are for each 10 s from 180340 to 180530 UT, except for the first two curves, whose times are as indicated. The dot gives the known values of N and B from Fig. 7 for 180510 UT. See text for details.

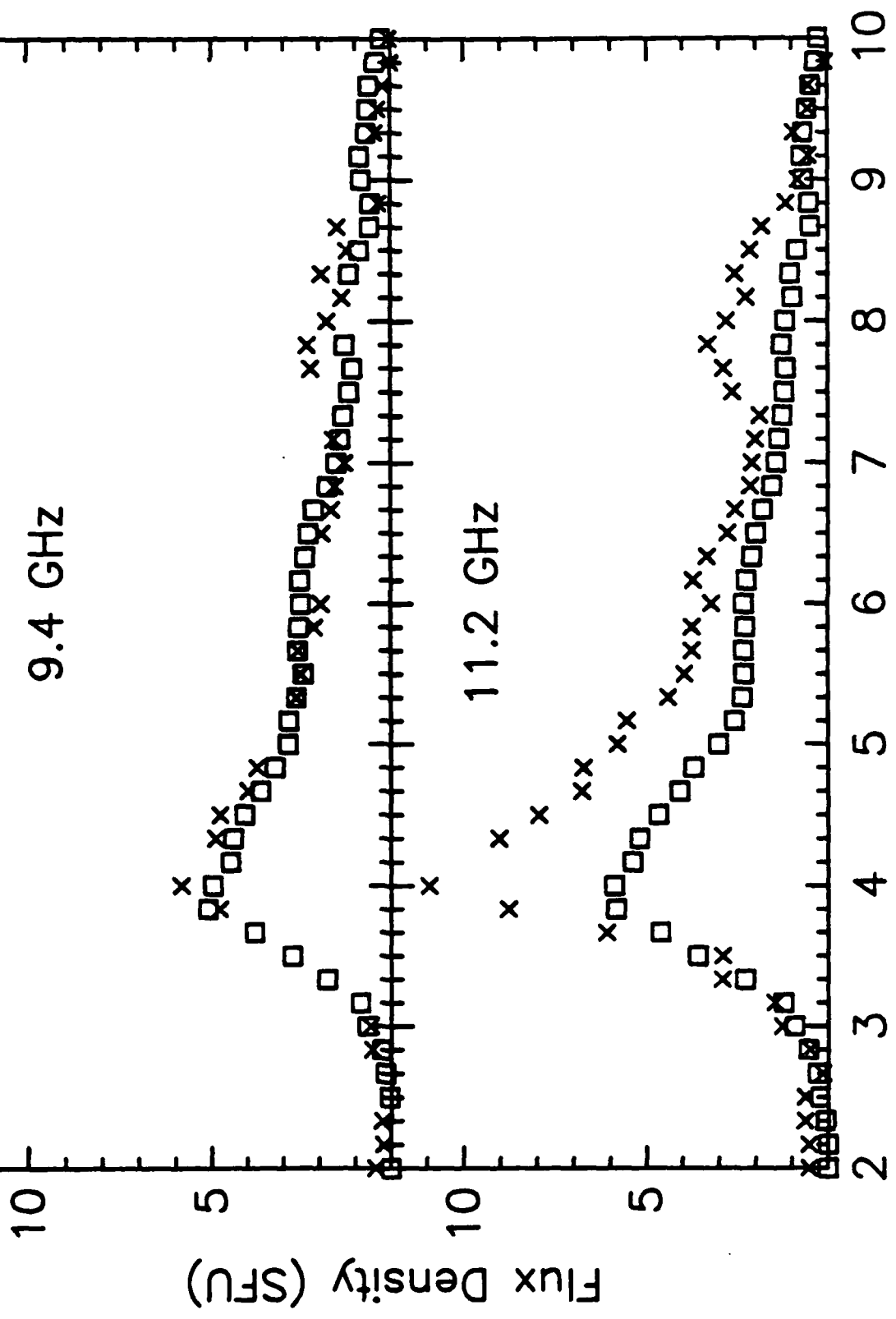
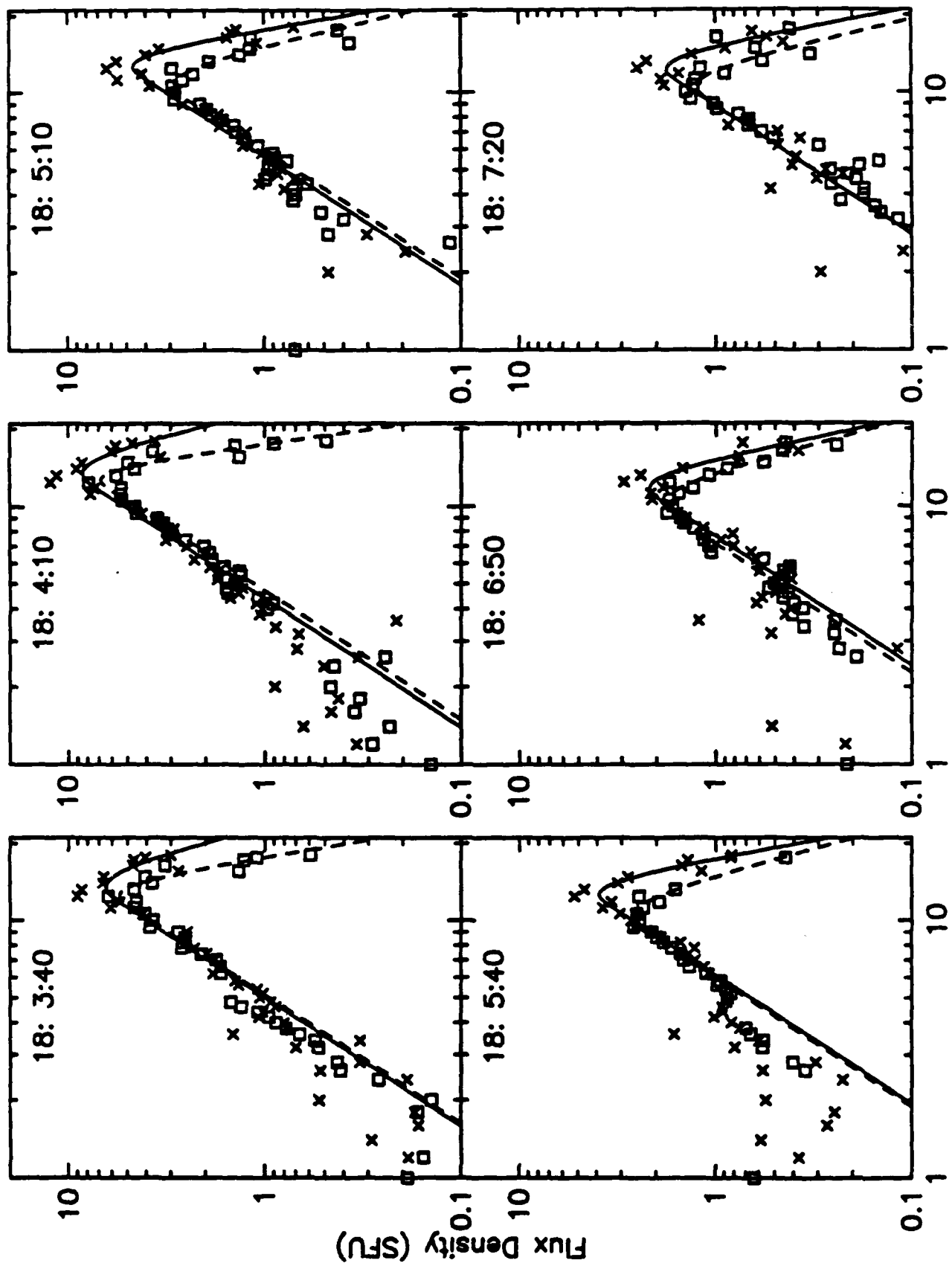


Figure 1
Time (min after 1800 UT)



Frequency (GHz)

Figure 2

Change in Source Size Near Peak of Flare

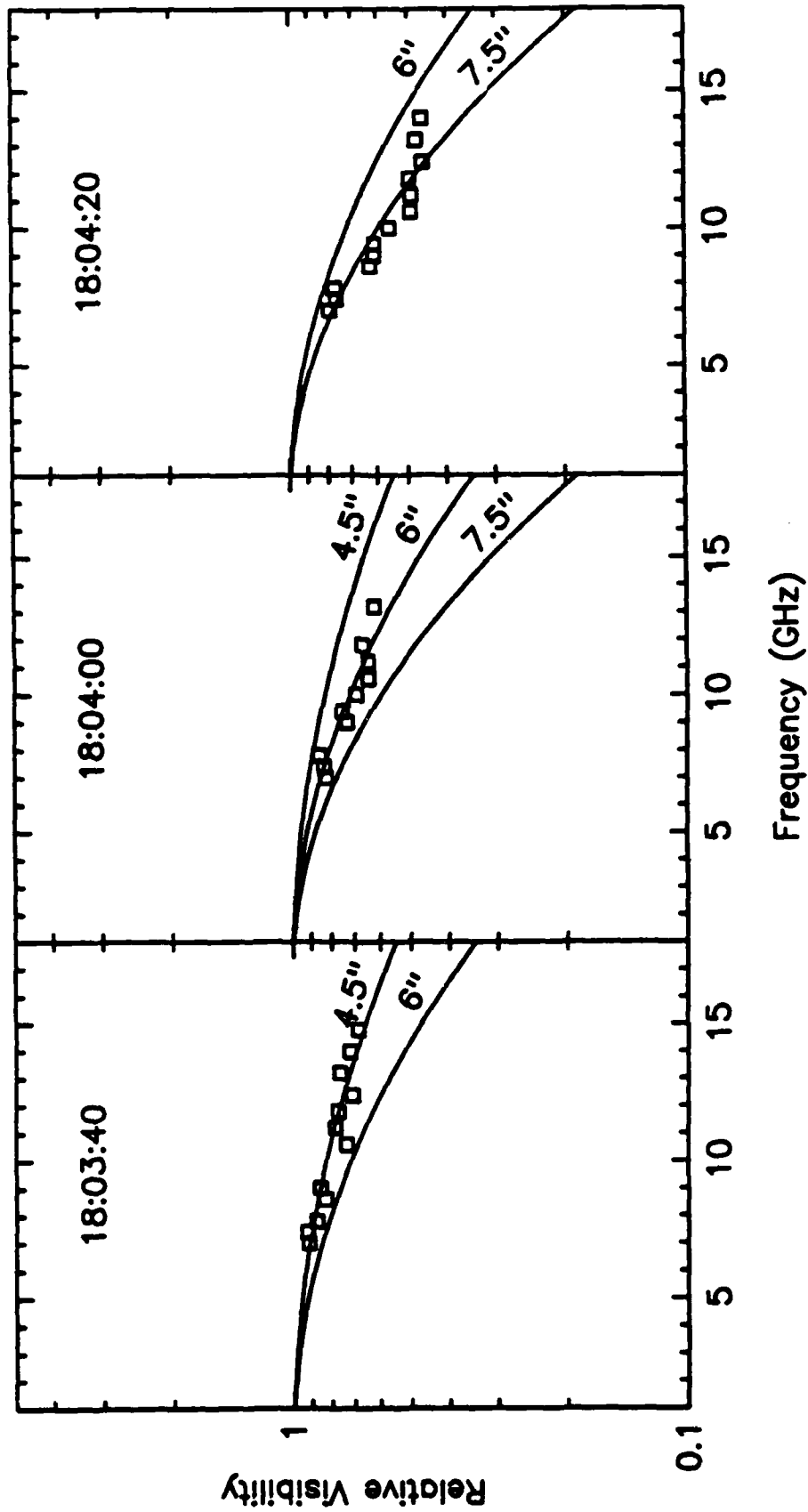
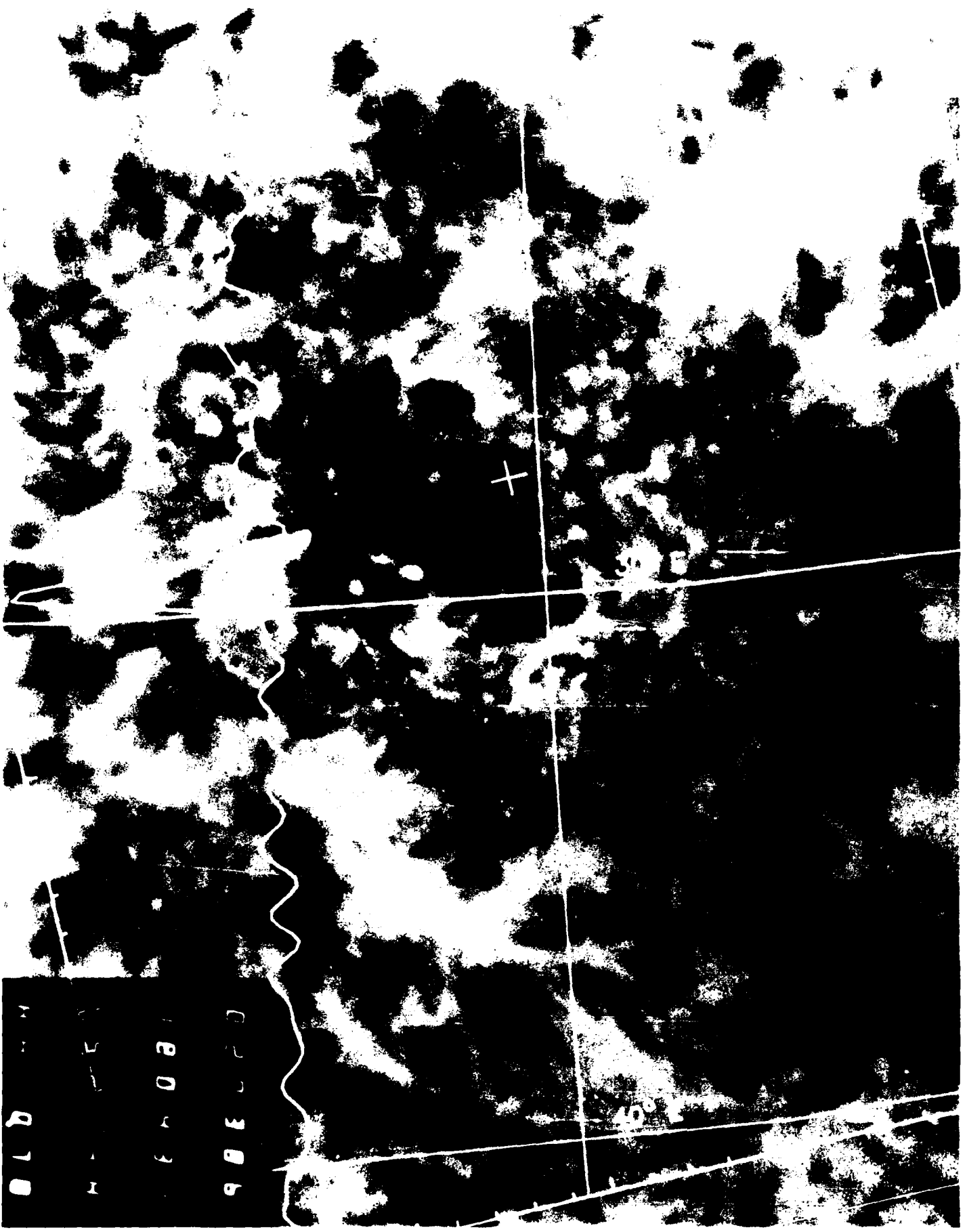


Figure 3

Q 70
18043
900306



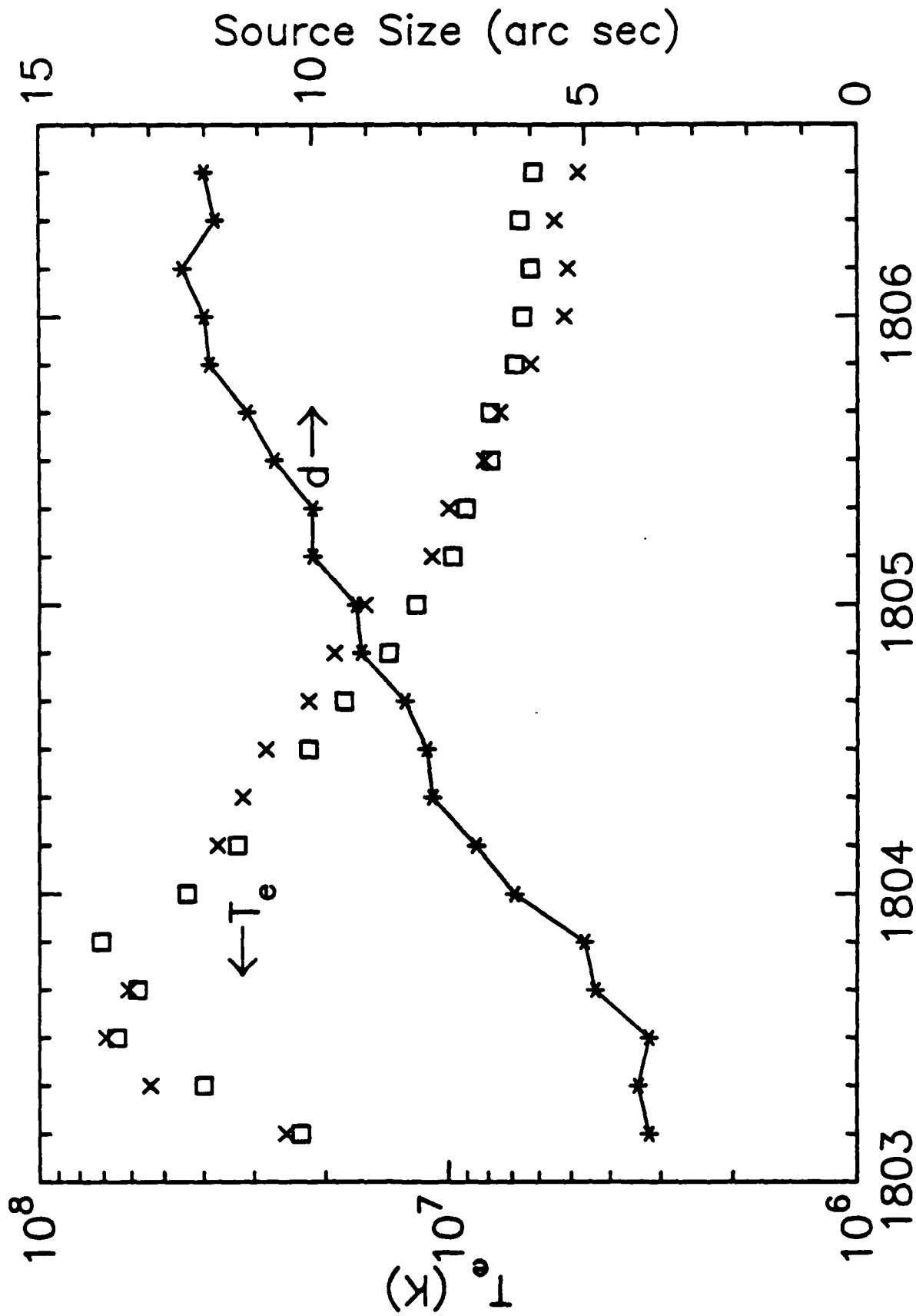
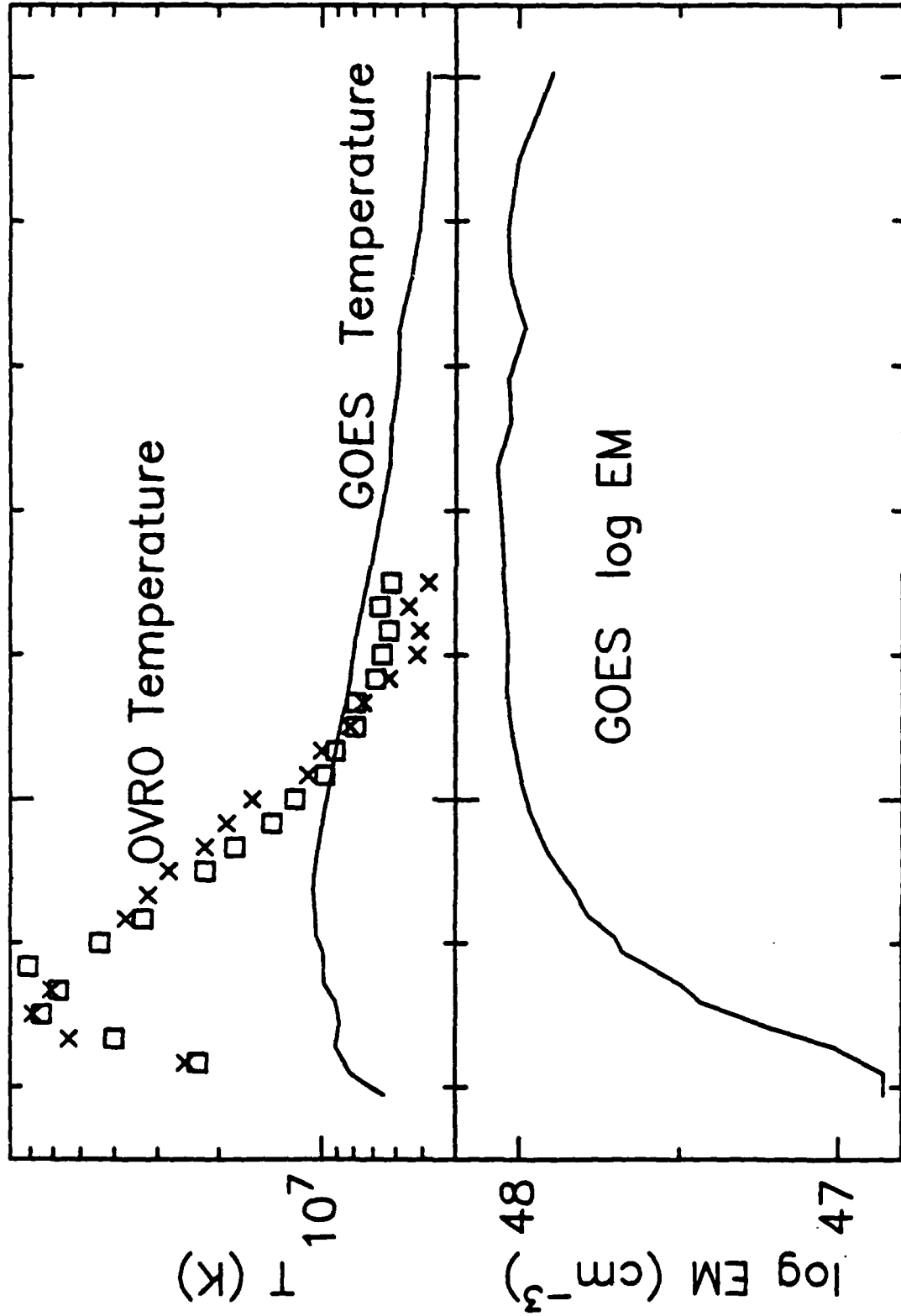


Figure 5



1810

1805

UT

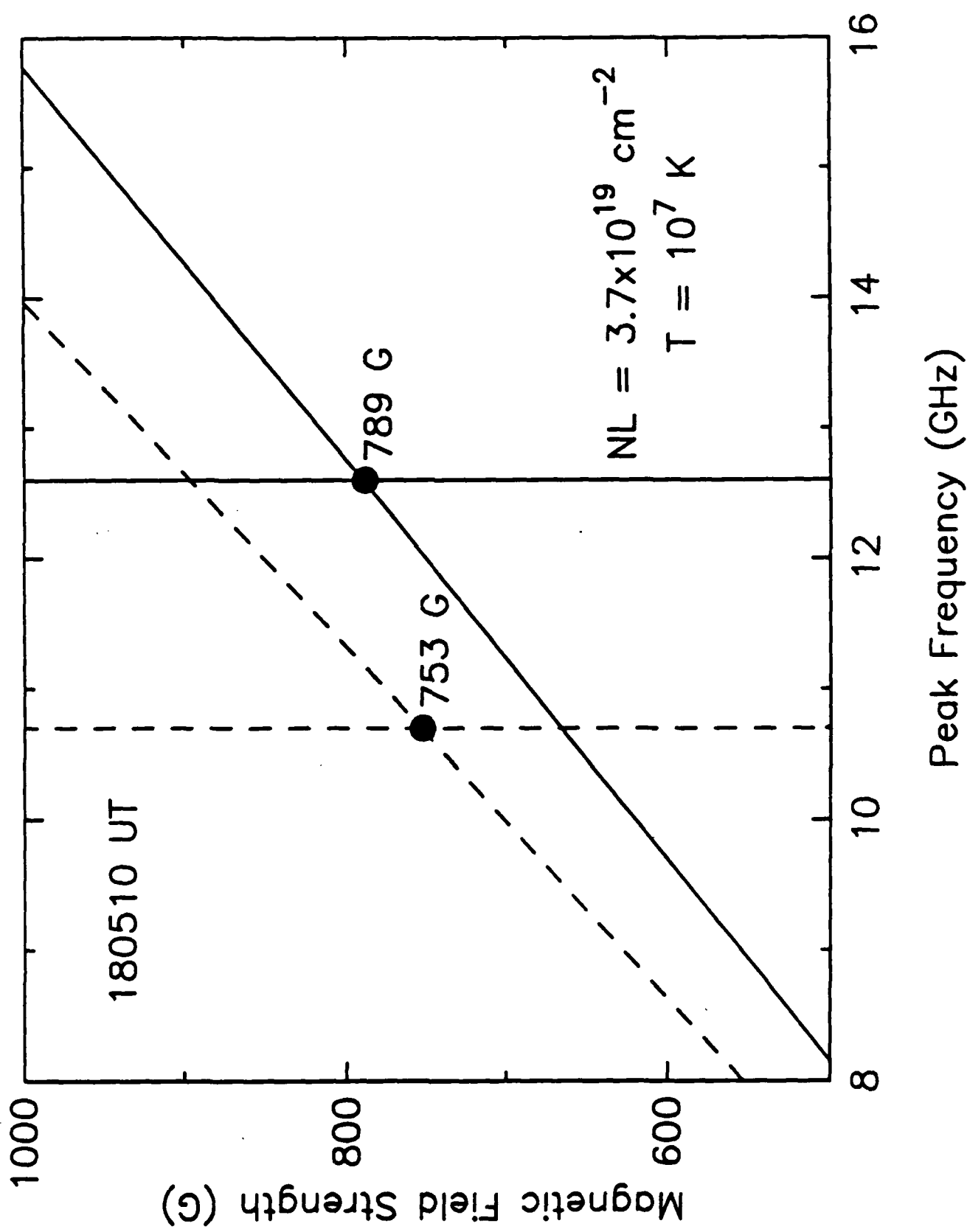
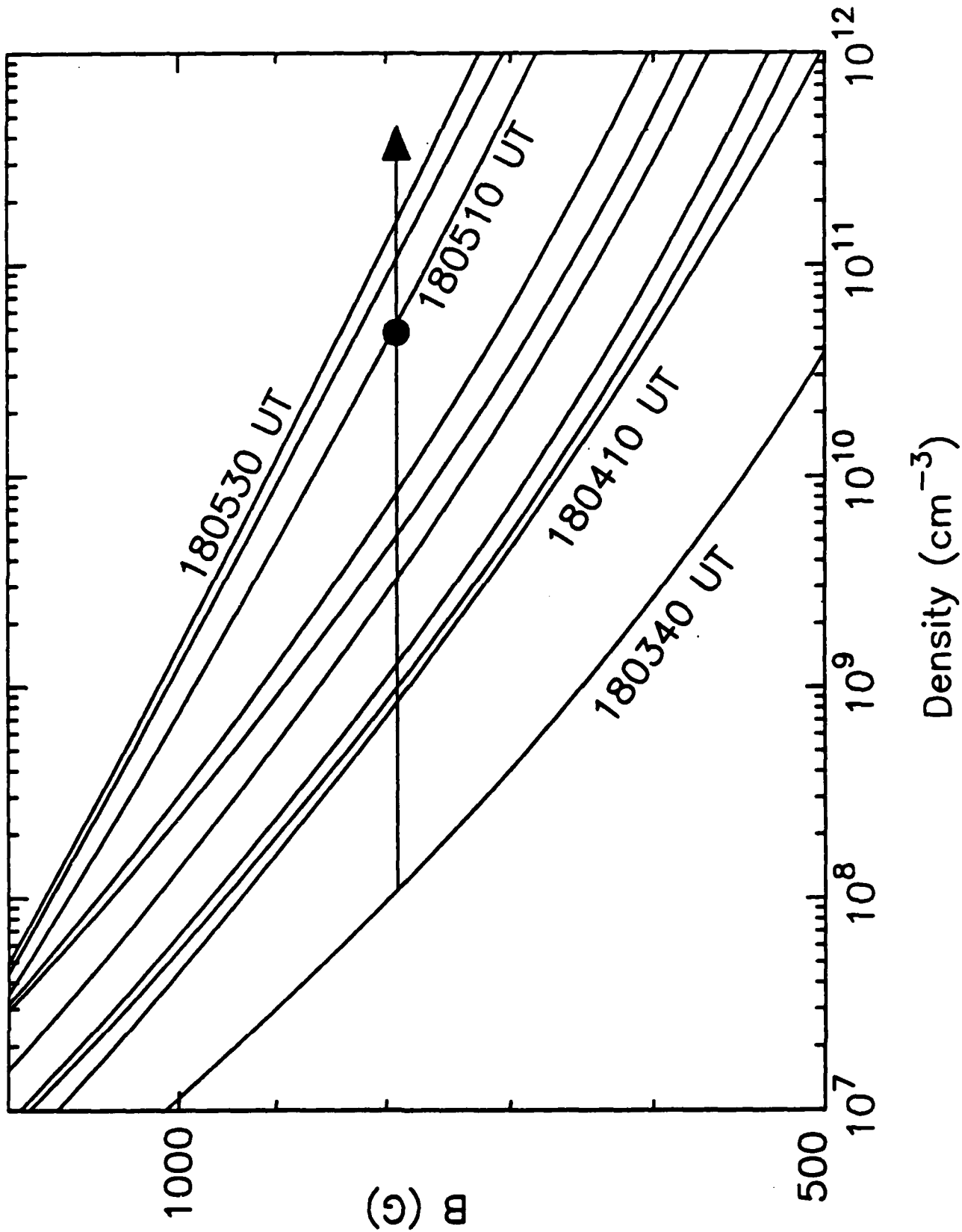


Figure 7



(c) B